



# Cerium, gallium and zinc containing mesoporous bioactive glass coating deposited on titanium alloy

S. Shruti\*, F. Andreatta, E. Furlani, E. Marin, S. Maschio, L. Fedrizzi

Università di Udine, Dipartimento Politecnico di Ingegneria e Architettura, Via del Cotonificio 108, 33100 Udine, Italy

## ARTICLE INFO

### Article history:

Received 23 November 2015  
Received in revised form 24 March 2016  
Accepted 28 March 2016  
Available online 30 March 2016

### Keywords:

Mesoporous bioactive glass with  $\text{Ce}_2\text{O}_3$   
 $\text{Ga}_2\text{O}_3$  or  $\text{ZnO}$   
 $\text{Ti6Al4V}$  substrate  
Polycaprolactone  
Dip coating  
*In vitro* bioactivity

## ABSTRACT

Surface modification is one of the methods for improving the performance of medical implants in biological environment. In this study, cerium, gallium and zinc substituted  $80\%\text{SiO}_2$ - $15\%\text{CaO}$ - $5\%\text{P}_2\text{O}_5$  mesoporous bioactive glass (MBG) in combination with polycaprolactone (PCL) were coated over  $\text{Ti6Al4V}$  substrates by dip-coating method in order to obtain an inorganic–organic hybrid coating (MBG-PCL). Structural characterization was performed using XRD, nitrogen adsorption, SEM-EDXS, FTIR. The MBG-PCL coating uniformly covered the substrate with the thickness found to be more than  $1\ \mu\text{m}$ . Glass and polymer phases were detected in the coating along with the presence of biologically potent elements cerium, gallium and zinc. In addition, *in vitro* bioactivity was investigated by soaking the coated samples in simulated body fluid (SBF) for up to 30 days at  $37\ ^\circ\text{C}$ . The apatite-like layer was monitored by FTIR, SEM-EDXS and ICP measurements and it formed in all the samples within 15 days except zinc samples. In this way, an attempt was made to develop a new biomaterial with improved *in vitro* bioactive response due to bioactive glass coating and good mechanical strength of  $\text{Ti6Al4V}$  alloy along with inherent biological properties of cerium, gallium and zinc.

© 2016 Elsevier B.V. All rights reserved.

## 1. Introduction

The surface properties of implants, especially those used to reconstruct damaged or diseased tissues are very important since their success depends on the biological interaction at the surface level. Coating and surface modification are some of the relevant methods by which the surface properties of the implant can be modified maintaining the bulk properties of the material [1]. Coating mainly provides (i) a shield to avoid toxic ion release from the implant, which could be harmful for human cells when exceed certain concentration values [2,3]. (ii) Compatible implant–tissue interface, which could provide good bonding between them helping to avoid implant failure [4].

Metallic implants are produced with different types of alloys including stainless steels, Co–Cr alloys and Ti-based alloys. In the field of orthopedic and dentistry, Ti-based alloys are gaining importance because among metallic implants it has the lowest elastic modulus. Thus, mechanical properties of Ti based alloys, such as  $\text{Ti6Al4V}$ , are closer to natural bone [5,6]. In addition, previous studies have shown that titanium based implants could be coated with

glass ceramics and/or calcium phosphate improving their bioactivity both *in vitro* and *in vivo* [7–9].

Recently, the application of organic–inorganic hybrid materials in the medical field has become an important research subject in order to induce a bioactive response in metallic implants. In particular, organic–inorganic hybrid materials can be successfully employed for coating metallic implants [10]. Polycaprolactone is a biodegradable, cost effective, synthetic, aliphatic polyester that has found wide applications in the field of biomaterials for different applications such as 3D scaffold preparation, hybrids for drug delivery, film substrates for tissue engineering, etc. [11–13]. However, PCL lacks effective bond formation with bone *in vivo* [14,15]. On the other hand, mesoporous bioactive glasses possess ordered mesoporous channel structure, high textural properties (surface area, pore volume and pore size), ability to induce quick apatite-like layer formation to form bond with bone and excellent cytocompatibility [16,17]. Incorporating biologically beneficial elements such as cerium, gallium and zinc into glass matrix can further improve MBG. *In vitro* study has shown positive effect of cerium on mouse osteoblasts and cerium oxide nanoparticles act as neuroprotective agents [18,19]. Gallium and zinc exhibit antimicrobial activity [20–23]. Furthermore, zinc has a stimulatory effect on bone formation [24].

\* Corresponding author.

E-mail address: [biotech.shruti@gmail.com](mailto:biotech.shruti@gmail.com) (S. Shruti).

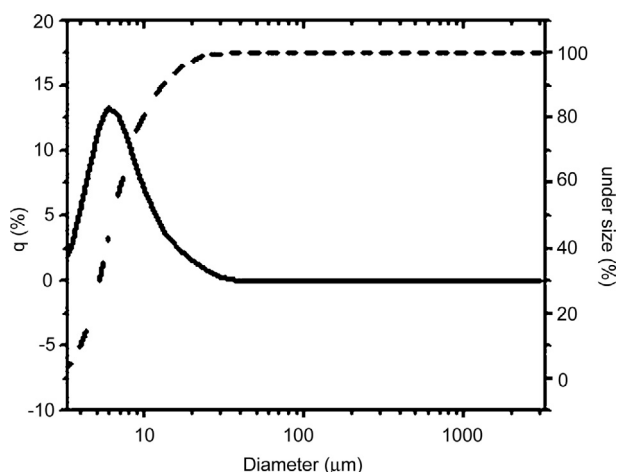


**Fig. 1.** Particle Size Distribution curve of blank MBG powder sample represented with logarithmic abscissa.

Previous studies on cerium, gallium and zinc doped 80%SiO<sub>2</sub>-15%CaO-5%P<sub>2</sub>O<sub>5</sub> (in mol.%) mesoporous bioactive glasses showed that they possess ordered mesoporous structure, optimum textural properties and *in vitro* bioactive response [25]. Further, they have also been tested as drug delivery system [26], 3D scaffolds [27], cytocompatibility and antibacterial ability [28].

In the present study, cerium, gallium and zinc substituted mesoporous bioactive glasses (MBG) and polycaprolactone (PCL) are employed for the deposition of organic–inorganic hybrid film produced by dip coating technique on Ti6Al4V alloy. The structure and chemical composition of the dip coatings were investigated with complementary techniques. In particular, the ability of the organic–inorganic hybrid coatings to form an apatite-like layer was evaluated by different techniques since this is a critical aspect in the view of possible application of hybrid coatings of to increase the bioactivity of Ti6Al4V alloy.

## 2. Materials and methods

### 2.1. Preparation of mesoporous bioactive glass

Ordered mesoporous (80-x)%SiO<sub>2</sub>-15%CaO-5%P<sub>2</sub>O<sub>5</sub> bioactive glass modified by xGa<sub>2</sub>O<sub>3</sub>, xCe<sub>2</sub>O<sub>3</sub>, xZnO, whose compositions are reported in Table 1, was synthesized using commercially available nonionic surfactant Pluronic® P123 (BASF) as a structure directing agent. P123 is an amphiphilic triblock copolymer having the sequence poly(ethylene oxide)-poly(propylene oxide)-poly(ethylene oxide) (PEO-PPO-PEO), EO<sub>20</sub>PO<sub>70</sub>EO<sub>20</sub>. The evaporation induced self-assembly (EISA) process was applied to synthesize bioactive mesoporous glasses.

During preparation, 4.5 g of Pluronic P123 was dissolved (~1 h) in 85 ml of ethanol with 1.12 ml of 0.5 N HNO<sub>3</sub>. At every 3 h interval, other reactants i.e., tetraethyl orthosilicate (TEOS), triethyl phosphate (TEP), calcium nitrate Ca(NO<sub>3</sub>)<sub>2</sub>·4H<sub>2</sub>O and cerium nitrate or gallium nitrate or zinc nitrate (Aldrich) were added under continuous stirring. The sol was poured in Petri dishes and kept at room temperature for 7 d. After the gelation process, the dried gels were removed as homogeneous and transparent membranes and calcinated at 700 °C for 3 h using heating rates of 2 °C min<sup>-1</sup>. The obtained glasses were subjected to attrition milling in order to obtain ~10 μm size particles to be employed in the dip coating method for the production of coated samples. All the blends (30 g of powder for each preparation) were homogenized by attrition milling for 1 h. Milling parameters are as follows: high-density

**Table 1**  
Composition of synthesized glasses (in mol.%).

Sample code	Samples	SiO <sub>2</sub>	CaO	P <sub>2</sub> O <sub>5</sub>	Substituent
Blank	80%SiO <sub>2</sub> -15%CaO-5%P <sub>2</sub> O <sub>5</sub>	80	15	5	–
Ce <sub>2</sub> O <sub>3</sub>	(80-x)%SiO <sub>2</sub> -15%CaO-5%P <sub>2</sub> O <sub>5</sub> - xCe <sub>2</sub> O <sub>3</sub>				1.0
Ga <sub>2</sub> O <sub>3</sub>	(80-x)%SiO <sub>2</sub> -15%CaO-5%P <sub>2</sub> O <sub>5</sub> - xGa <sub>2</sub> O <sub>3</sub>				1.0
ZnO	(80-x)%SiO <sub>2</sub> -15%CaO-5%P <sub>2</sub> O <sub>5</sub> - xZnO				2.0

**Table 2**  
Textural properties of blank, cerium, gallium and zinc substituted mesoporous bioactive glass.

Samples	S <sub>BET</sub> (m <sup>2</sup> g <sup>-1</sup> )	Pore size (nm)	Pore volume (cm <sup>3</sup> g <sup>-1</sup> )
Blank	354	4.1	0.426
1.0%Ce <sub>2</sub> O <sub>3</sub>	266	3.5	0.282
1.0%Ga <sub>2</sub> O <sub>3</sub>	309	4.0	0.376
2.0%ZnO	313	3.5	0.319

nylon container (volume = 750 ml); 500 g of 99 wt.% alumina balls (diameter = 6–8 mm); 100 ml of ethanol (98%); 300 cycles min<sup>-1</sup>.

After milling, particle size distribution (PSD) was evaluated using a Horiba LA950 laser scattering PSD analyzer. The measurements were carried out in water after sonication for 3 min. For clarity of comprehension PSD curves are represented with logarithmic abscissa, as it is commonly done for the presentation of this type of results.

### 2.2. Dip coating

Ti6Al4V discs of dimension 30 mm diameter and 2 mm thickness were used as substrate for the deposition of organic–inorganic hybrid coatings. Before dip coating, the substrates were subjected to pretreatments consisting of grinding with 800 grit silicon carbide (SiC) emery paper followed by etching in Kroll's reagent for 1 min. The Kroll's reagent is a hydrous solution comprising of 6 ml nitric acid (HNO<sub>3</sub>) and 2 ml hydrofluoric acid (HF) dissolved in 92 ml distilled water. Different surface preparation methods were considered including only grinding or grinding and etching with different immersion times in the Kroll's reagent. The procedure reported above is the one that optimized the adhesion behavior of the hybrid coatings on the substrate. After pretreatment, the substrates were cleaned ultrasonically in water, acetone and ethanol for 10 min each and dried at room temperature for 24 h.

Milled MBG powder (2 g) was suspended in 37 ml of dichloromethane (DCM) with the aid of ultrasound for 30 min. Simultaneously, 2.6 g of polycaprolactone (PCL) was dissolved in 37 ml of dichloromethane by magnetic stirring at room temperature for 40 min. Later, MBG powder suspended in dichloromethane was added in completely dissolved PCL–dichloromethane solution. This mixture was allowed to evaporate by magnetic stirring and temperature was maintained by keeping the paste in water bath at 25–30 °C. Independent of chemical composition of a paste, the right consistency for coating was obtained in 2 h corresponding to solid to liquid (g/ml) ratio of the suspension ~1:8. Subsequently, Ti6Al4V alloy substrates were dipped into PCL–ceramic slurry with withdrawal speed of 300 mm min<sup>-1</sup> for 2 cycles and dried at room temperature for 1 d. The coating parameters were optimized by testing set of withdrawal speed and number of cycles for dipping. It was kept in mind that the thickness of the film should be able to form apatite-like layer after SBF treatment and remain intact on the surface of the substrate.

### 2.3. In vitro bioactivity test

Bioactivity test was carried out by keeping coated sample in simulated body fluid (SBF) solution. Each sample was soaked in

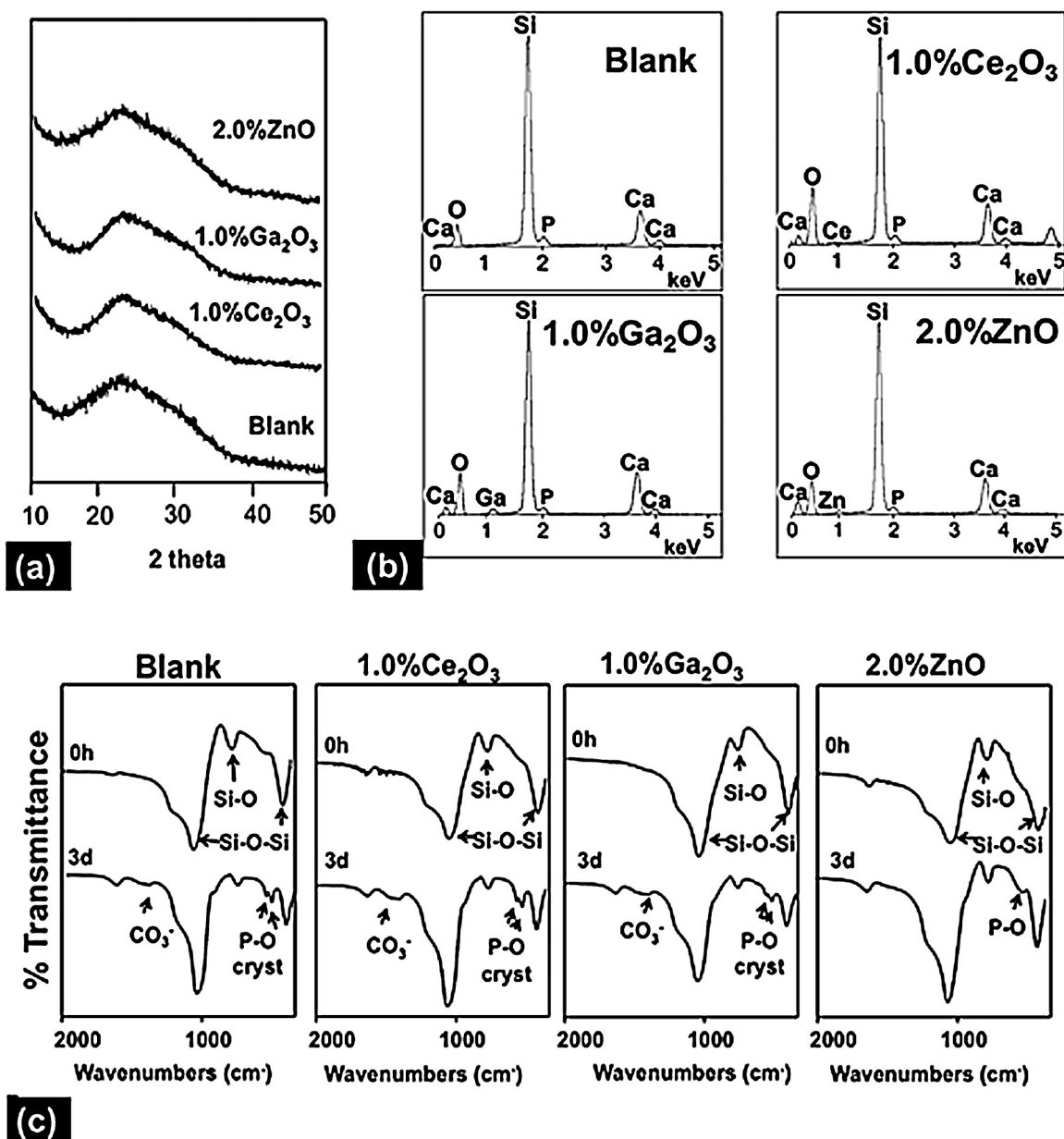


Fig. 2. (a) XRD pattern, (b) EDXS image and (c) FTIR spectra (before and after soaking in SBF for 3 d) of blank, cerium, gallium and zinc MBG powder samples.

SBF for five different time intervals (1 d, 3 d, 7 d, 15 d, 30 d) in 30 ml of SBF at 37 °C [29]. The SBF solution was filtered with a 0.22 μm Milipore® system filter to avoid bacterial contamination. The samples were kept in such a way that they were completely submerged in SBF. The study was performed in static condition where SBF was not changed throughout the experiment. After soaking at 37 °C for different time periods the samples were removed from the SBF solution and washed first in distilled water and then in ethanol for 2 s each. Later samples were dried for 24 h at room temperature. The chemical composition of the SBF solution and changes in the concentration of calcium, phosphorus, silicon, cerium, gallium and zinc during the *in vitro* bioactivity tests were analyzed by an ICP spectrometer (ICP Optima 4200DV, Perkin Elmer).

#### 2.4. Characterization

Powder X-ray diffraction experiments were performed with a Philips X'Pert diffractometer (equipped with real time multiple strip detector) operated at 40 kV and 40 mA using Ni-filtered Cu

Kα radiation. XRD patterns were collected using a step size of 0.03° and a counting time of 50 s per angular abscissa in the 2θ range between 5° and 55°.

Textural characteristics were measured according to the BET method by nitrogen adsorption at 77 K, using Tristar 3000 gas adsorption analyzer (Micromeritics). Before the adsorption measurement, the samples were degassed under vacuum for 1 h at 150 °C.

FTIR analyses of glass surfaces were carried out in Jasco FT/IR-4200 spectrometer using KBr pellets. To prepare KBr pellet, 249 mg of KBr and 1 mg of sample was mixed properly.

Microstructures of the coated samples were examined by a Zeiss EVO40 scanning electron microscope (SEM) coupled with the energy dispersive X-ray spectroscopy (EDXS) to evaluate the microstructure of the coatings as well as the final content of silicon, calcium, phosphorus, cerium, gallium and zinc in each sample. Before analysis, samples were coated with gold for 2 cycles (each of 20 s) at 0.12 mA and 30 mbar.

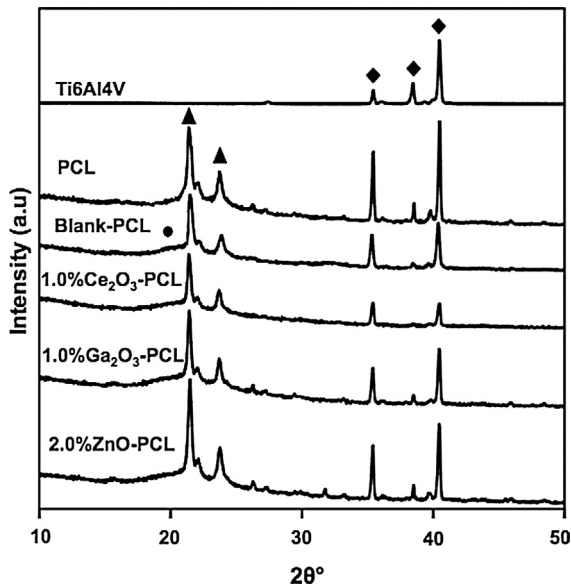


Fig. 3. XRD pattern of PCL and blank, cerium, gallium, zinc MBG after mixing with PCL. (Amorphous silica matrix) ●; (PCL peaks) ▲; (Ti peaks) ◆.

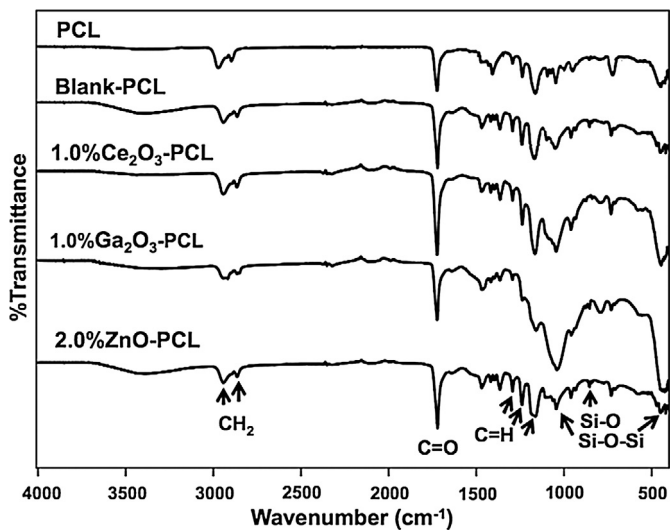


Fig. 4. FTIR spectra of PCL and blank, cerium, gallium, zinc MBG after mixing with PCL.

### 3. Results and discussion

The PSD of the powders used for the dip coating procedure must be distributed within a narrow and possibly micronic range [30]. Fig. 1 shows the PSD curve of the 80%SiO<sub>2</sub>-15%CaO-5%P<sub>2</sub>O<sub>5</sub> powder sample, which was selected as representative of all blends after the milling procedure. A monomodal PSD centered at 7 μm can be observed, with minimum particles size close to 1 μm and maximum at about 20 μm. All the other blends, displayed PSD curves similar to that reported above after the milling procedure. Therefore, it is assumed that, as a result of attrition milling, all compositions investigated in this work display similar behavior during the dip coating procedure.

Before proceeding with coating, the milled cerium, gallium and zinc MBG powder samples were examined by XRD, nitrogen adsorption, EDXS and *in vitro* bioactivity test. Fig. 2(a) reports the XRD patterns of blank, cerium, gallium and zinc substituted MBG powder. The amorphous structure of the silica matrix of MBG was

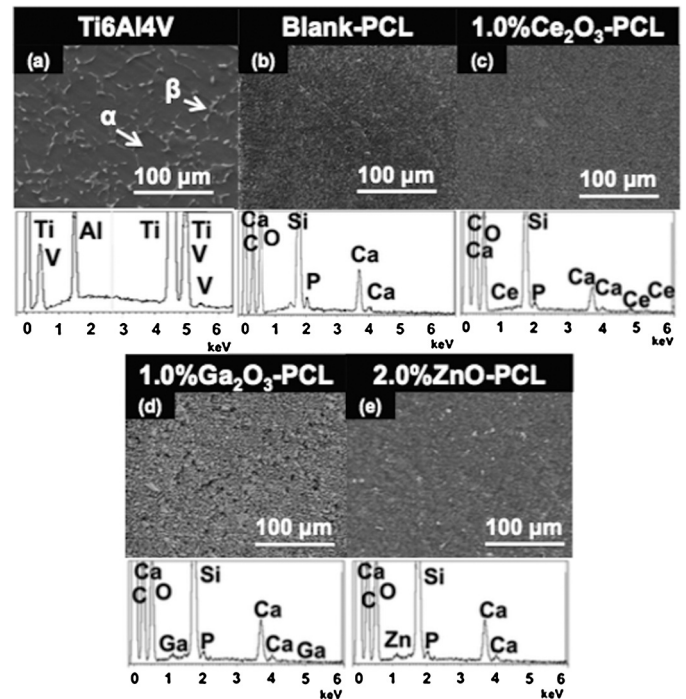


Fig. 5. SEM-EDXS results of Ti6Al4V substrate (a) uncoated and (b–e) coated with blank, cerium, gallium and zinc MBG-PCL.

confirmed by the presence of a broad band between 20 and 30° (2θ value) with no diffraction maxima in all the samples. Table 2 displays the specific surface area ( $S_{BET}$ ), pore volume and pore size of the samples. The specific surface area ranges from 266 m<sup>2</sup> g<sup>-1</sup> for Ce containing glass to 354 m<sup>2</sup> g<sup>-1</sup> for the blank sample. Pore size ranges from 3.5 nm for Ce and Zn containing glasses to 4.1 nm for the blank sample, whereas pore volume ranges from 0.282 cm<sup>3</sup> g<sup>-1</sup> for Ce containing glass to 0.426 cm<sup>3</sup> g<sup>-1</sup> for the blank sample. The textural properties of attrition milled glasses reported were similar to those observed in previous research [25]. The EDXS analysis carried out on the milled MBG powder samples (Fig. 2(b)) shows homogenous distribution of substituents as well as silicon, calcium and phosphorus. The FTIR spectra (Fig. 2(c)) of the blank, 1.0%Ce<sub>2</sub>O<sub>3</sub>, 1.0%Ga<sub>2</sub>O<sub>3</sub> and 2.0%ZnO mesoporous glasses show intense absorption bands at 1040 and 470 cm<sup>-1</sup> that correspond to the asymmetric bending vibration of the Si–O bond and a band at 800 cm<sup>-1</sup> that is attributed to symmetric stretching of the Si–O bond. After 3 d of SBF soaking in the SBF solution, absorption bands of crystalline calcium phosphate at 560 and 600 cm<sup>-1</sup> were present along with carbonate band at 1419 cm<sup>-1</sup> indicating apatite-like layer formation. These absorption bands were detected in all samples except 2.0%ZnO MBG, in line with results reported in previous study [25]. The results obtained on MBG powder samples confirm that the glasses prepared in this work retain their physical, chemical and *in vitro* properties after attrition milling.

The powder samples consisting of cerium, gallium and zinc substituted mesoporous bioactive glasses and polycaprolactone (indicated as “MBG-PCL”) were successively employed for the deposition of organic–inorganic hybrid films by dip coating technique on Ti6Al4V substrates according to the procedure reported above.

Fig. 3 displays the X-ray diffraction patterns of uncoated Ti6Al4V substrate, PCL and blank, cerium, gallium, zinc substituted MBG-PCL coated titanium samples. The XRD patterns for all coated samples were very similar. The broad hump between 20 and 30° (2θ value) was due to the amorphous silica matrix, which indicates presence of ceramic in the coating on the substrate. The

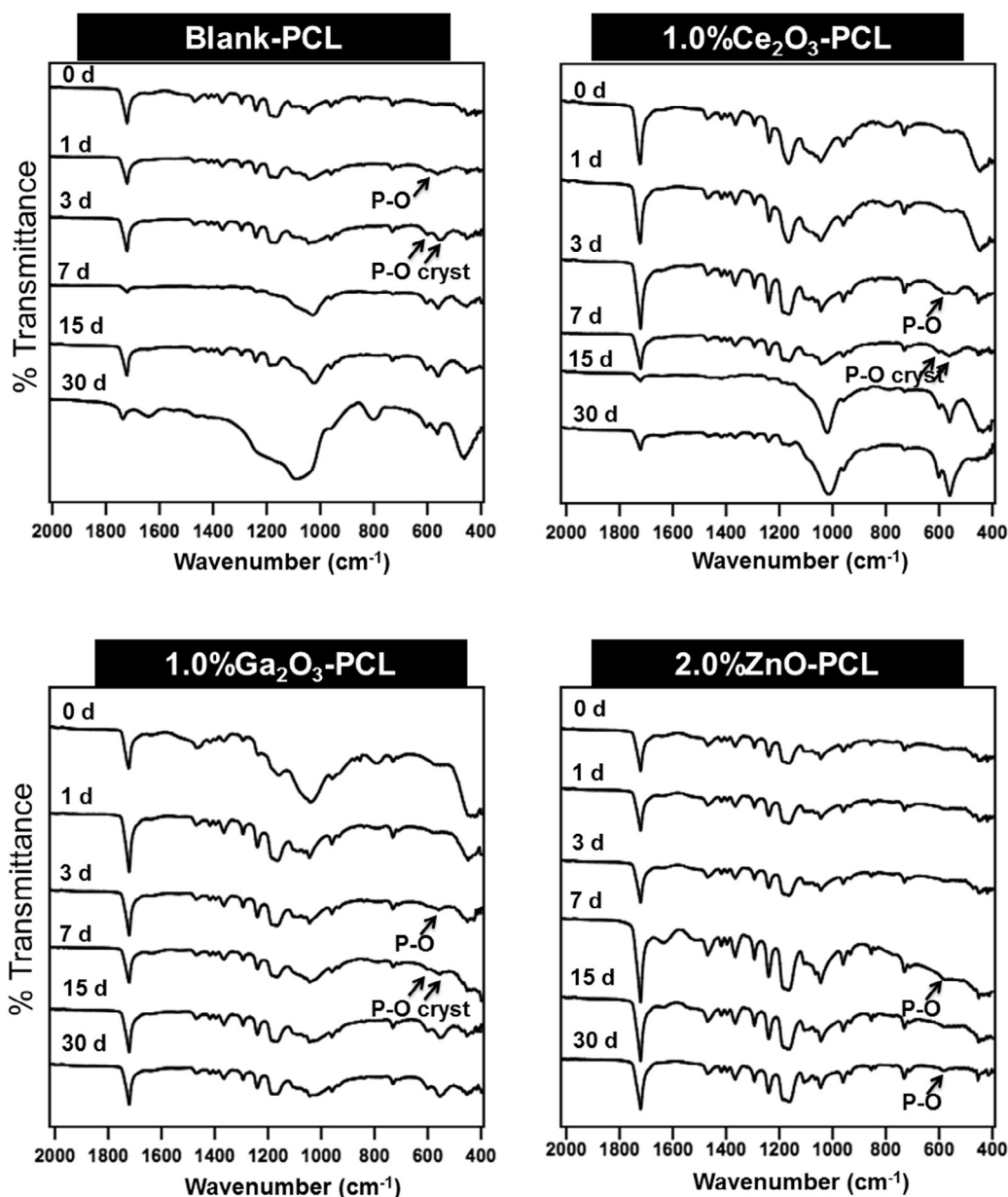


Fig. 6. FTIR spectra of blank, cerium, gallium and zinc MBG-PCL coating before and after soaking in SBF for different time intervals.

hump in PCL was not well defined. In addition, the sharp peaks typical of crystalline material visible in the diffractogram were of PCL and titanium [31,32]. The FTIR spectra (see Fig. 4) of PCL and blank, cerium, gallium, zinc MBG-PCL show characteristic bands of  $-\text{CH}_2-$  at  $2950$  and  $2853\text{ cm}^{-1}$ ,  $\text{C}=\text{O}$  at  $1720\text{ cm}^{-1}$  and carboxylic group at  $1250$  and  $1170\text{ cm}^{-1}$  for polycaprolactone, respectively [33,34]. Furthermore, the absorption band at  $1035$  and  $442\text{ cm}^{-1}$  are assigned to the  $\text{Si}-\text{O}-\text{Si}$  asymmetric stretch and the band centered at  $\sim 800\text{ cm}^{-1}$  could be ascribed to  $\text{Si}-\text{O}$  symmetric stretch [35]. These bands were not present in PCL samples.

Fig. 5 presents the surface morphology of the uncoated and those of blank, cerium, gallium, zinc substituted MBG-PCL coated titanium substrates. The uncoated titanium substrate (see Fig. 5(a)) showed the alpha and beta phases of titanium as a result of grinding and etching in the Kroll's reagent. Adhesion of the coating is due to combination of surface roughness formed by grinding and successive etching in the Kroll's reagent. The SEM micrograph image of coated Ti6Al4V alloy substrates (see Fig. 5(b)–(e)) showed that the organic–inorganic hybrid film deposited by dip coating uniformly

cover the substrate and are crack free. This suggests a good adhesion between the coating and substrate. Moreover, the coatings present a heterogeneous structure comprising of random sized particles with sharp edges, which is typical for a mesoporous bioactive glass. The thickness of the coating was found to be more than  $1\text{ }\mu\text{m}$  measured by fracturing the film and mounting the side on in SEM. It is within the required limits of apatite layer formation. EDXS analysis showed (see Fig. 5(b)–(e)) homogeneous distribution of Si, Ca, P, and C in the coated samples. Moreover, Ce, Ga, Zn introduced in the coatings can be detected by EDXS analysis. These results together with those obtained by XRD and FTIR on MBG-PCL coatings confirm the presence of an organic–inorganic hybrid structure consisting of both glass and polymer phases.

### 3.1. In vitro bioactivity test

Bioactive materials exhibit significant feature of bonding with living bone through apatite-like layer formation on its surface when in contact with physiological fluid both *in vitro* and *in vivo*. *In vitro*

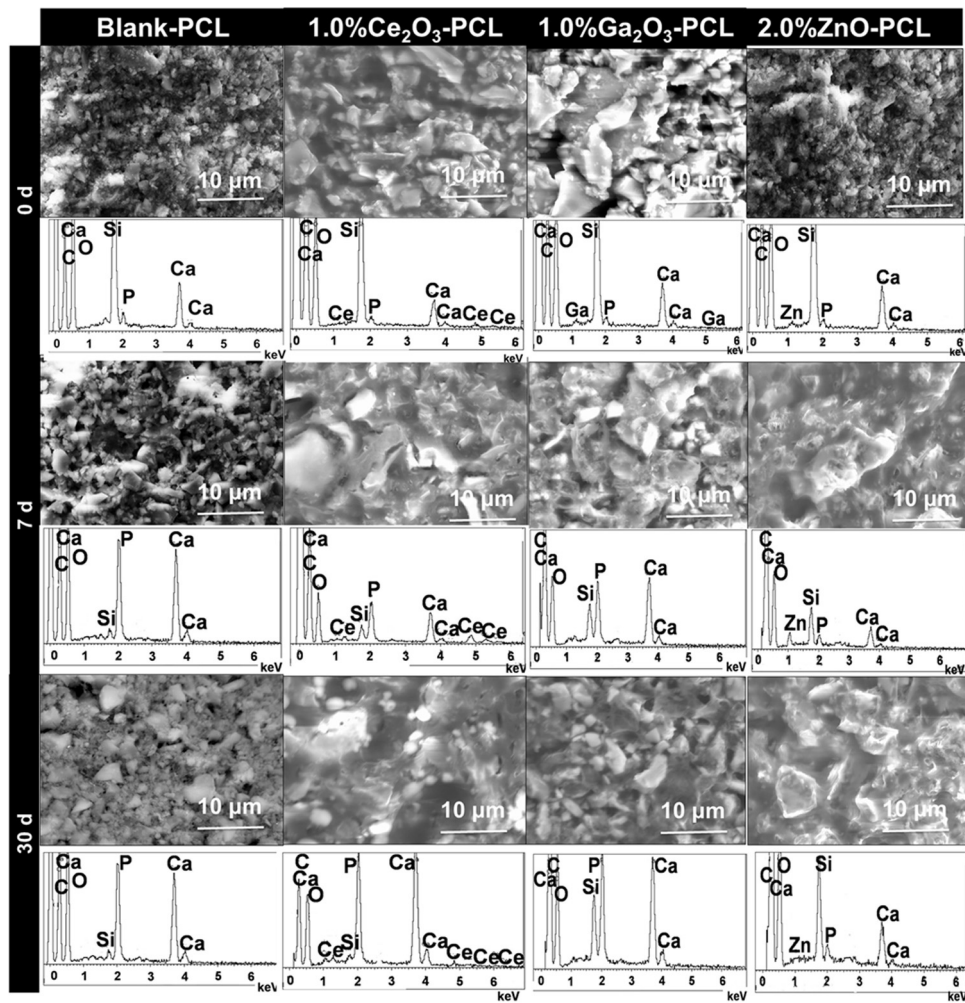


Fig. 7. SEM-EDXS results of blank, cerium, gallium and zinc MBG-PCL coating before and after soaking in SBF showing evolution of hydroxyapatite surface layer formation.

bioactivity assay can be performed by soaking bioactive materials in a fluid (simulated body fluid) mimicking human plasma [29]. Bacterial contamination is avoided by filtering the simulated body fluid (SBF) before soaking the samples. During the assay, rapid exchange of cations like  $\text{Ca}^{2+}$  ions from the glass and  $\text{H}_3\text{O}^+$  of the solution takes place. This results in formation of Si–OH group on the glass surface forming nucleation sites for apatite layer. Later,  $\text{Ca}^{2+}$  and  $\text{PO}_4^{3-}$  from solution precipitates on the nucleation site to form amorphous calcium phosphate layer, which eventually crystallizes to form apatite-like layer by incorporation of  $\text{OH}^-$  and  $\text{CO}_3^{2-}$  anions from the solution. In the present study, the formation of apatite layer was monitored by two ways—directly by analyzing the apatite formation on the surface of the coated substrates by FTIR and SEM-EDXS and indirectly by evaluating changes in calcium, phosphorus and silicon concentration in SBF solution.

Fig. 6 shows the FTIR spectra of blank, cerium, gallium and zinc MBG-PCL coated titanium substrates before and after soaking in SBF for six different time intervals (0 h, 1 d, 3 d, 7 d, 15 d and 30 d). After 1 d of soaking, the absorption band at  $561\text{ cm}^{-1}$  was observed corresponding to an amorphous phosphate in blank MBG-PCL coated sample. In 1.0%Ce<sub>2</sub>O<sub>3</sub> and 1.0%Ga<sub>2</sub>O<sub>3</sub> MBG-PCL coated samples same band was recorded but after 3 d of SBF immersion. A well-resolved doublet at  $560$  and  $600\text{ cm}^{-1}$  corresponding to crystalline calcium phosphate was found in blank MBG-PCL coated sample after 3 d [36]. On the other hand, beginning of doublet formation was observed in 1.0%Ce<sub>2</sub>O<sub>3</sub> and 1.0%Ga<sub>2</sub>O<sub>3</sub> substituted MBG-PCL coated samples, except in 2.0%ZnO, after 7 d of soaking. In 2.0%ZnO

MBG-PCL coated sample, the intensity of phosphate band increased with soaking time with no doublet formation even after 30 d. This clearly indicates that all samples show *in vitro* bioactive response except 2.0%ZnO MBG-PCL.

Fig. 7 shows SEM-EDXS analysis of blank, 1.0%Ce<sub>2</sub>O<sub>3</sub>, 1.0%Ga<sub>2</sub>O<sub>3</sub> and 2.0%ZnO substituted MBG-PCL coated samples before and during SBF treatment. The results clearly depict high *in vitro* bioactivity shown by blank, 1.0%Ce<sub>2</sub>O<sub>3</sub> and 1.0%Ga<sub>2</sub>O<sub>3</sub> MBG-PCL coated titanium samples. Before soaking, a large amount of Si and small amounts of Ca and P were detected in EDXS spectra. After 7 d of SBF immersion, significantly high concentrations of Ca and P and a small amount of Si were found in the newly formed surface layer. This was further confirmed by checking the Ca/P molar ratio value 1.64 by 7 d, which is in the range of the calcium deficient biological apatite [37]. On the other hand, in case of 2.0%ZnO MBG-PCL coating Ca and P amount did not increase even after 30 d of SBF soaking hence showing low *in vitro* bioactivity response.

Change in SBF composition during *in vitro* bioactivity tests can be used as an indirect method to understand the events that take place on the glass surface. Partial soluble nature of bioactive glass causes increase in Ca, P and Si ions in solution. Later on Ca and P level of SBF solution decreases due to calcium phosphate layer formation on the surface of glass. In the present study, variations in Ca, P and Si value of SBF solution were monitored during *in vitro* bioactivity assays (see Fig. 8). It can be seen that Ca level increased in blank MBG-PCL sample till 1 d and then the level starts to decrease. Similar trends were observed in 1.0%Ce<sub>2</sub>O<sub>3</sub> and 1.0%Ga<sub>2</sub>O<sub>3</sub> MBG-

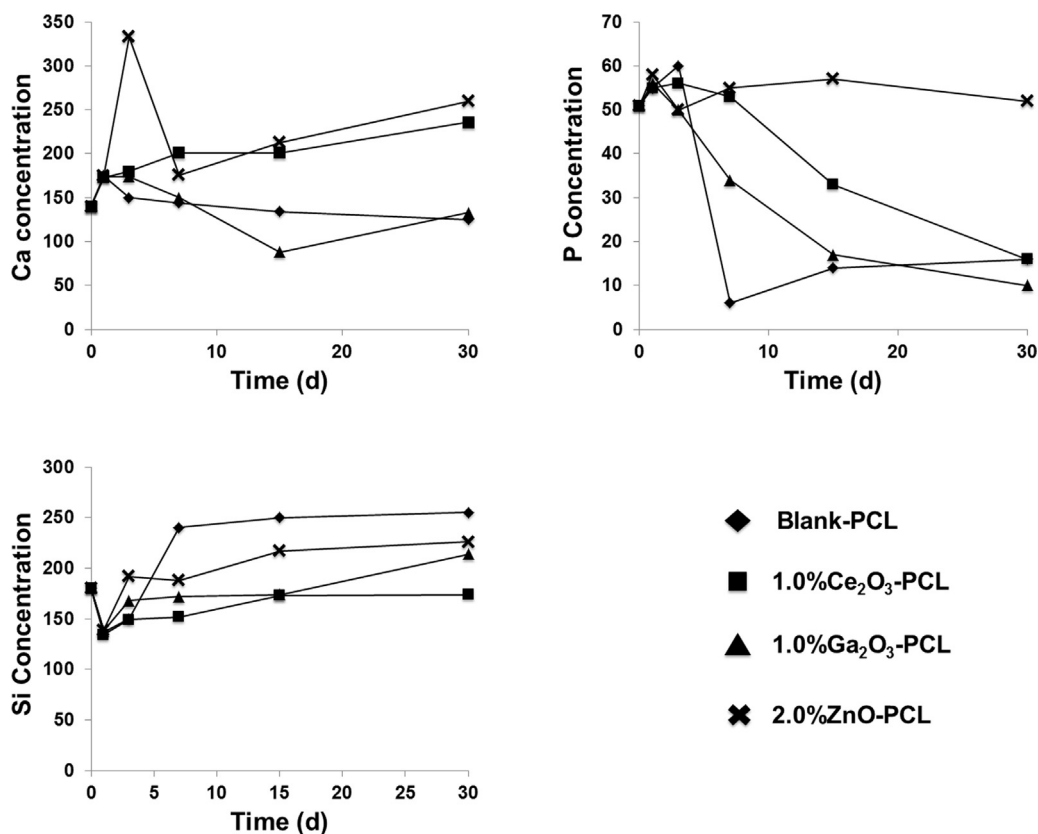


Fig. 8. Variation in concentration of calcium, phosphorus and silicon with soaking time in SBF.

PCL coated samples in which the increase of Ca ion was detected within 3 d, although it decreases for longer soaking time.

Profile of P concentration was quite similar for blank, 1.0%Ce<sub>2</sub>O<sub>3</sub> and 1.0%Ga<sub>2</sub>O<sub>3</sub> MBG-PCL coated samples where it increased till 1 d and then decreased as a function of time to ~10 ppm. The Si concentration in all the samples showed increase in level after 1 d of SBF soaking.

On the other hand, 2.0%ZnO MBG-PCL coated sample displayed a different behavior as compared to the other compositions. Initial increment in Ca, P and Si level was recorded along with only slight fluctuation in their concentration till 30 d. Previous studies have shown that zinc in glass composition improved chemical durability, slowed down the formation rate of calcium phosphate layer and decreased the size of crystalline apatite particles [38].

During *in vitro* bioactivity assay, the pH of SBF solution remained fairly constant for 30 d. After 1 d, only slight change was observed from 7.4 to 7.8. Thereafter, it remained constant throughout the assay.

This study has demonstrated that cerium, gallium and zinc substituted 80%SiO<sub>2</sub>-15%CaO-5%P<sub>2</sub>O<sub>5</sub> mesoporous bioactive glass can be coated on Ti6Al4V alloy by combining with polycaprolactone. Our next objective will be to study the coated sample in cell culture to verify if they maintain the desired biological properties induced by substitution.

#### 4. Conclusions

In the present study, hybrid coating containing cerium, gallium and zinc substituted 80%SiO<sub>2</sub>-15%CaO-5%P<sub>2</sub>O<sub>5</sub> mesoporous bioactive glass and polycaprolactone were deposited on Ti6Al4V alloy by dip coating method. Cerium, gallium and zinc exhibit important role in bone metabolism like positive effect on primary osteoblasts, improve mechanical properties of bone, stimulatory effect on bone

formation, respectively. The obtained coating was homogenous and crack free having thickness more than 1 μm which is enough to initiate apatite-like layer formation. This was confirmed by *in vitro* bioactivity assay where blank, 1.0%Ce<sub>2</sub>O<sub>3</sub> and 1.0%Ga<sub>2</sub>O<sub>3</sub> MBG-PCL coated samples maintained optimum *in vitro* response. However, 2.0%ZnO MBG-PCL sample showed negative *in vitro* response, which could be due to the improved chemical durability by zinc in glass composition that slows down the apatite-like layer formation. Hence, blank, 1.0%Ce<sub>2</sub>O<sub>3</sub> and 1.0%Ga<sub>2</sub>O<sub>3</sub> MBG-PCL coatings deposited on Ti6Al4V alloy samples combine the good *in vitro* bioactivity typical of bulk MBG of same composition with the structural properties of Ti6Al4V titanium alloy.

#### Acknowledgements

Financial support through European Social Fund (project DIANET- incoming mode) is gratefully acknowledged. The authors wish to thank Prof. L. Menabue, Prof. G. Lusvardi and Dr. G. Malvasi of the University of Modena and Reggio Emilia for instrument availability and assistance.

#### References

- [1] M. Catauro, F. Bollino, P. Veronesi, G. Lamanna, Influence of PCL on mechanical properties and bioactivity of ZrO<sub>2</sub>-based hybrid coatings synthesized by sol-gel dip coating technique, *Mater. Sci. Eng. C Mater. Biol. Appl.* 39 (2014) 344–351.
- [2] S.A. Brown, L. Farnsworth, K. Merrit, T.D. Crowe, In vitro and in vivo metal ion release, *J. Biomed. Mater. Res.* 22 (1988) 321–338.
- [3] M. Long, H.J. Rack, Titanium alloys in total joint replacement—a materials science perspective, *Biomaterials* 19 (1998) 1621–1639.
- [4] N. Hijon, M. Manzano, A.J. Salinas, M. ValletRegi, Bioactive CaO-siO<sub>2</sub>-PDMS coating on Ti6Al4V substrate, *Chem. Mater.* 17 (2005) 1591–1596.
- [5] M.R. Pilliar, G.C. Weatherly, Developments in implant alloys, *CRC Crit. Rev. Biocompat.* 1 (1984) 371–403.

- [6] J.B. Brunski, *Biomaterials Science*, in: B.D. Ratner (Ed.), Academic Press, San Diego, CA, 1996, pp. 37–130.
- [7] A.M. Piccirillo, S.S. Borysenko, S.D. Borysenko, Qualitative analysis behavior of the solutions of impulsive differential systems, *Atti. Accad. Pelor. Pericol. Cl. Sci. Fis. Mat. Nat.* 89 (2011), <http://dx.doi.org/10.1478/C1A8902002>.
- [8] A.M. Piccirillo, M. Ciarletta, S.D. Borysenko, Impulsive wendroff's type inequalities and their applications, *Atti. Accad. Pelor. Pericol. Cl. Sci. Fis. Mat. Nat.* 90 (2012), <http://dx.doi.org/10.1478/AAPP.902A2>.
- [9] R. Gupta, A. Kumar, Bioactive materials for biomedical applications using sol-gel technology, *Biomed. Mater.* 3 (2008), <http://dx.doi.org/10.1088/1748-6041/3/3/034005>.
- [10] J. Livage, T. Coradin, C. Roux, *Functional Hybrid Materials*, in: P. Gomez-Romero, C. Sanchez (Eds.), Wiley-VCH, Weinheim, Germany, 2004, pp. 387–404.
- [11] D.W. Huttmacher, T. Schantz, I. Zein, K. Woei Ng, S. HinTeoh, K. Cheng Tan, Mechanical properties and cell cultural response of polycaprolactone scaffolds designed and fabricated via fused deposition modeling, *J. Biomed. Mater. Res.* 55 (2001) 203–216.
- [12] H.L. Khor, K.W. Ng, J.T. Schantz, T. ThangPhan, T.C. Lim, S.H. Teoh, D.W. Huttmacher, Polycaprolactone films as a potential substrate for tissue engineering an epidermal equivalent, *Mater. Sci. Eng. C* 20 (2002) 71–75.
- [13] M. Catauro, F. Bollino, Anti-inflammatory entrapment in polycaprolactone/silica hybrid material prepared by sol-gel route characterization, bioactivity and in vitro release behavior, *J. Appl. Biomater. Funct. Mater.* 11 (2013) 172–179.
- [14] Y.F. Zhou, V. Sae-Lim, A.M. Chou, D.W. Huttmacher, T.M. Lim, Does seeding density affect in vitro mineral nodules formation in novel composite scaffolds? *J. Biomed. Mater. Res. A* 78 (2006) 183–193.
- [15] V.V. Seregin, J.L. Coffey, Biomaterialization of calcium disilicide in porous polycaprolactone scaffolds, *Biomaterials* 27 (2006) 4745–47–54.
- [16] D. Arcos, M. Vallet-Regi, Sol-gel silica based biomaterials and bone tissue regeneration, *Acta Biomater.* 6 (2010) 2874–2888.
- [17] W. Zhai, H. Lu, L. Chen, X. Lin, Y. Huang, K. Dai, K. Naoki, G. Chen, J. Chang, Silicate bioceramics induce angiogenesis during bone regeneration, *Acta Biomater.* 8 (2012) 341–349.
- [18] J. Zhang, C. Liu, Y. Li, J. Sun, P. Wang, K. Di, Y. Zhao, Effect of cerium ion on the proliferation, differentiation and mineralization function of primary mouse osteoblasts in vitro, *J. Rare Earth* 28 (2010) 138–142.
- [19] D. Schubert, R. Dargusch, J. Raitano, S.W. Chan, Cerium and yttrium oxide nanoparticles are neuroprotective, *Biochem. Biophys. Res. Commun.* 342 (2006) 86–91.
- [20] R.S. Bockman, A.L. Boskey, N.C. Blumenthal, N.W. Alcock, R.P. Warrell Jr., Gallium increase bone calcium and crystallite perfection of hydroxyapatite, *Cacif Tissue Int.* 39 (1986) 376–381.
- [21] T.J. Hall, T.J. Chamber, Gallium inhibits bone resorption by a direct effect on osteoclast, *Bone Miner.* 8 (1990) 211–216.
- [22] J.R. Harrington, R.J. Martens, N.D. Cohen, L.R. Bernstein, Antimicrobial activity of gallium against virulent *Rhodococcus equi* in vitro and in vivo, *J. Vet. Pharmacol. Ther.* 29 (2006) 121–127.
- [23] S.B. Aydin, L. Hanley, Antimicrobial activity of dental composites containing zinc oxide nanoparticles, *J. Biomed. Mater. Res. B: Appl. Biomater.* 94 (2010) 22–31.
- [24] A. Ito, H. Kawamura, M. Otsuka, M. Ikeuchi, H. Ohgushi, K. Ishikawa, K. Onuma, N. Kanzaki, Y. Sogo, N. Ichinose, Zinc releasing calcium phosphate for stimulating bone formation, *Mater. Sci. Eng. C* 22 (2002) 21–25.
- [25] A.J. Salinas, S. Shruti, G. Malavasi, L. Menabue, M. Vallet-Regi, Substitutions of cerium, gallium and zinc in ordered mesoporous bioactive glasses, *Acta Biomater.* 7 (2011) 3452–3458.
- [26] S. Shruti, A.J. Salinas, E. Ferrari, G. Malavasi, G. Lusvardi, A.L. Doadrio, L. Menabue, M. Vallet-Regi, Curcumin release from cerium, gallium and zinc containing mesoporous bioactive glasses, *Micropor. Mesopor. Mat.* 180 (2013) 92–101.
- [27] S. Shruti, A.J. Salinas, G. Lusvardi, G. Malavasi, L. Menabue, M. Vallet-Regi, Microporous bioactive scaffolds prepared with cerium, gallium and zinc containing glasses, *Acta Biomater.* 9 (2013) 4836–4844.
- [28] S. Sanchez-Salcedo, S. Shruti, A.J. Salinas, G. Malavasi, L. Menabue, M. Vallet-Regi, In vitro antibacterial capacity and cytocompatibility of SiO<sub>2</sub>-CaO-P<sub>2</sub>O<sub>5</sub> meso-macroporous glass scaffolds enriched with ZnO, *J. Mater. Chem. B* 2 (2014) 4836–4847.
- [29] T. Kokubo, H. Takadama, How useful is SBF in predicting in vivo bone bioactivity, *Biomaterials* 27 (2006) 2907–2915.
- [30] N. Barth, C. Schilde, A. Kwade, Influence of particle size distribution on micro mechanical properties of the thin nanoparticulate coatings, *Physics Procedia* 40 (2013) 9–18.
- [31] H.W. Kim, J.C. Knowles, H. Kim, Hydroxyapatite/polycaprolactone composite coating on hydroxyapatite porous bone scaffolds for drug delivery, *Biomaterials* 25 (2004) 1279–1287.
- [32] C. Wu, Y. Ramaswamy, D. Gale, W. Yang, K. Xiao, L. Zhang, Y. Tin, H. Zreiqat, Novel sphere coatings on Ti-6Al-4 V for orthopedic implants using sol-gel method, *Acta Biomater.* 4 (2008) 569–576.
- [33] D. Verma, K. Katti, D. Katti, Experimental investigation of interfaces in hydroxyapatite/polyacrylic acid/polycaprolactone composites using photoacoustic FTIR spectroscopy, *J. Biomed. Mater. Res. A* 77 (2006) 59–66.
- [34] H.W. Kim, J.C. Knowles, H.E. Kim, Effect of biphasic calcium phosphates on drug release and biological and mechanical properties of polycaprolactone composite membranes, *J. Biomed. Mater. Res. A* 70 (2004) 467–479.
- [35] Z.L. Hua, J.L. Shi, L. Wang, W.H. Zhang, Preparation of mesoporous silica films on a glass slide surfactant template removal by solvent extraction, *J. Non-Cryst. Solids* 292 (2001) 177–183.
- [36] M. Vallet-Regi, I. Izquierdo-Barba, A.J. Salinas, Influence of P<sub>2</sub>O<sub>5</sub> on crystallinity of apatite formed in vitro on surface of bioactive glass, *J. Biomed. Mater. Res.* 46 (1999) 560–565.
- [37] S. Shruti, A.J. Salinas, G. Malavasi, G. Lusvardi, L. Menabue, C. Ferrara, P. Mustarelli, M. Vallet-Regi, Structural and in vitro study of cerium, gallium and zinc containing sol-gel bioactive glasses, *J. Mater. Chem.* 22 (2012) 13698–13706.
- [38] F. Baghbani, F. Maztarzadeh, L. Hajibaki, M. Mozafari, Synthesis, characterization and evaluation of bioactivity and antibacterial activity of quinary glass system (SiO<sub>2</sub>-CaO-P<sub>2</sub>O<sub>5</sub>-MgO-ZnO): In vitro study, *Bull. Mater. Sci.* 36 (2013) 1339–1346.